Advances in Differential Equations and Control Processes 2025, 32(1), 2799.
https://doi.org/10.59400/adecp2799

Article

Rolling optimization control method for hydro-photovoltaic-storage microgrid based on stochastic chance constraints

Qianjin Gui[1,*], Wenfa Xu[1], Xiaoyang Li[1], Lirong Luo[1], Haifeng Ye[2], Zhengfeng Wang[2]

[1] State Grid Anhui Electric Power Co., Ltd. Anqing Power Supply Company, Anqing 246000, China
[2] State Grid Anhui Electric Power Co., Ltd., Hefei 230000, China
*** Corresponding author:** Qianjin Gui, qianjin_gui@126.com

CITATION

Gui Q, Xu W, Li X, et al. Rolling optimization control method for hydro-photovoltaic-storage microgrid based on stochastic chance constraints. Advances in Differential Equations and Control Processes. 2025; 32(1): 2799. https://doi.org/10.59400/adecp2799

ARTICLE INFO

Received: 18 February 2025
Accepted: 3 March 2025
Available online: 11 March 2025

Abstract: Hydro-photovoltaic-storage (HPS) microgrid has gradually become an important measure to optimize the energy structure and ensure the reliability of regional power supply. However, due to the strong randomness and spatiotemporal correlations of hydropower and photovoltaic (PV) output, traditional deterministic optimization methods are difficult to support the accurate regulation and reliable operation of microgrid with a high proportion of renewable energy integration. On this basis, a rolling optimization control method for HPS microgrid based on stochastic chance constraints is proposed. A novel multivariate scenario reduction method considering hydro-PV correlations is presented to characterize the uncertainty of renewable energy output, and a day-ahead stochastic optimal scheduling model based on chance-constrained programming is constructed. Combined with stochastic model predictive control strategies, the day-ahead scheduling plan can be adjusted at multiple time scales, both intraday power compensation and real-time adjustments, to suppress the intraday power fluctuations induced by day-ahead scenario errors and reduce the influence of the uncertainty of hydro-PV power output on microgrid operation. Experimental results show that compared with the traditional deterministic scheduling method, the proposed method can effectively improve the stability and economy of HPS microgrid operation under complex uncertain conditions.

Keywords: hydro-photovoltaic-storage microgrid; stochastic optimal scheduling; correlated uncertainties; multivariate scenario reduction; model predictive control

1. Introduction

In recent years, driven by the construction of new power systems with renewable energy as the main component, the proportion of renewable energy integrated into the grid has gradually increased, significantly alleviating the energy crisis. The hydro-photovoltaic-storage (HPS) microgrid is a new multi-energy complementary power generation system that combines hydropower, photovoltaic (PV) power generation, and energy storage technology, which is an effective way to promote renewable energy consumption, improve energy utilization efficiency, and reduce energy costs [1,2]. However, the strong randomness in hydropower and PV output severely restricts the operational reliability of the microgrid and its support to the regional distribution network. Therefore, optimizing the operation of HPS microgrids under uncertain conditions is crucial for enhancing the power supply reliability and the overall economic benefits of the system.

Compared to the traditional deterministic optimization scheduling methods based on point forecasts, microgrid stochastic optimization scheduling represents the statistical distribution characteristics of renewable sources and loads through a series

of discrete scenarios. It can flexibly address the adverse effects of source-load uncertainty on microgrid scheduling while avoiding the risks brought by the single deterministic decisions as much as possible [3–6]. In Rezaee Jordehi et al. [7], a tri-level stochastic operational planning framework based on renewable energy scenarios was developed for isolated microgrids with hydrogen refueling station integrated energy hubs. In Azizivahed et al. [8], scenario-based stochastic programming was used to handle the uncertainty of wind-solar output in reconfigurable multi-microgrids, and both technical and economic aspects of the microgrid system were improved significantly. To increase the robustness of system operation, Seyedeh-Barhagh et al. [9] and Shaillan et al. [10] proposed the risk-aware stochastic optimal energy management models for the microgrids with PV and wind generation. In Hu and Li [11], a transfer learning-based scenario generation method was adopted to characterize the uncertainty of multiple wind energy sources for the stochastic optimal scheduling of a microgrid with newly built wind farms. Wu et al. [12] presented an improved spectral clustering method for scenario reduction of renewable energy in the stochastic optimal dispatching of the electricity-hydrogen-gas-heat integrated energy system. In Abunima et al. [13], a two-stage stochastic optimization algorithm considering the potential future PV profile in a probability density function form was proposed, which can decrease the operation cost compared to the conventional optimization method considering the worst-case scenarios. Li et al. [14] addressed the uncertainty of wind-solar output in microgrids by constructing a stochastic optimal scheduling model to minimize operating costs and, combined with Conditional Value-at-Risk (CVaR), avoided most risk losses with minimal cost. Jani et al. [15], a two-stage optimization model was established for the stochastic day-ahead and real-time energy management of networked microgrids considering the integration of renewable sources. Moreover, multi-stage stochastic optimization models considering the uncertainty of PV output were proposed to enhance the security of the power supply of microgrids in Aaslid et al. [16] and Kizito et al. [17].

Although the scenario-based stochastic scheduling method is widely used for uncertainty modeling of renewable energy to improve the accuracy of decision results and achieve reliable microgrid operations in uncertain environments, it requires generating a great number of scenarios for decision-making. The number of scenarios increases exponentially with the increase of the scheduling stage, greatly increasing the time costs and solving difficulty. In this aspect, Heitsch and Römisch [18] developed the famous probability distance-based scenario reduction methods, namely fast forward selection (FFS) and simultaneous backward reduction (SBR), which have been adopted to improve the solving efficiency of various practical scheduling problems [19–21]. In Beltran et al. [22], a multistage scenario reduction method based on quadratic process distance was presented for solving the stochastic medium-term hydrothermal scheduling problem. Zhan et al. [23] presented an improved Kantorovich distance-based forward selection method to shorten the time consumption of scenario reduction. Considering the correlations between the renewable energy sources, Hu and Li [24], Hu and Li [25] developed the comprehensive optimal scenario reduction model to minimize the partial correlation loss and maximize the probabilistic similarity degree after the reduction operation. However, existing scenario reduction methods cannot simultaneously preserve the

spatial and temporal correlations of renewable sources, which will have a significant impact on the decision-making reliability and accuracy for HPS microgrid scheduling.

Considering the impact of source-load uncertainty on the stable operation of microgrids, model predictive control (MPC), which adjusts the original plan through rolling optimization and feedback correction, has been widely applied in microgrid optimization scheduling. Zhang et al. [26], Bazmohammadi et al. [27] considered the randomness of loads and the uncertainty of wind-solar output, combining MPC with scenario analysis methods, and proposed an optimization scheduling strategy for microgrids based on stochastic MPC. Jiao et al. [28] adopted robust stochastic MPC with different granularity models to handle source-load uncertainty and established a two-stage optimal scheduling framework for microgrids, improving computational efficiency and economic performance. Lin et al. [29], Wei et al. [30] developed the scenario-based stochastic model predictive control approach for microgrid operation under uncertainties to balance the computational efficiency, robustness and economy of the scheduling results. However, although extensive studies have been conducted on the optimal scheduling of microgrids under uncertain conditions, there are relatively few studies that simultaneously consider the uncertainty of hydropower and PV output, especially the spatial and temporal correlations between hydro-PV power output. Moreover, the existing studies on the optimization scheduling of HPS microgrids only focused on the day-ahead scheduling stage, without considering the impact of scenario errors on the scheduling results. In the actual scheduling process, the real-time changes in hydro-solar power output and user loads will affect the stability and economic operation of HPS microgrids, which still requires further research.

In light of the above, the main contributions of this paper are summarized as follows:

(1) A multi-timescale rolling optimization control method for an HPS microgrid based on stochastic model predictive control is proposed. In the day-ahead scheduling stage, a stochastic optimal scheduling model for the HPS microgrid based on chance-constrained programming is constructed to obtain a reference scheduling plan. Based on a stochastic model predictive control strategy, a closed-loop scheduling is conducted through rolling optimization and feedback correction across multiple time scales, including intraday power compensation optimization and real-time power adjustments. Experimental results indicate that the proposed method can not only minimize the power fluctuations caused by day-ahead scenario errors but also effectively suppress the impact of hydro-PV power uncertainty on the stable and economic operation of the HPS microgrid.

(2) To improve the solving efficiency of HPS microgrid scheduling models, a multivariate scenario reduction method considering the correlations between hydro-PV output is proposed. It aims to maximize the probability similarity of the original scenario sets and the preserved scenario set, and minimize the temporal and spatial correlation loss of hydro-PV output scenarios before and after scenario reduction. A comprehensive optimal scenario reduction model is constructed, and the overall process of iterative scenario reduction is provided based on the optimal redistribution rule. The simulation results show that the proposed method can preserve the statistical

characteristics of the reduced scenario to the greatest extent possible, and effectively improve the decision reliability and accuracy of HPS microgrid scheduling.

The rest of this paper is organized as follows: In Section 2, a multi-time scale optimal scheduling model for the HPS microgrid is proposed, and the stochastic MPC strategy involved in the rolling optimization process is also presented. The multivariate scenario reduction method considering spatiotemporal correlations among sources is developed in Section 3. The experimental results are discussed in Section 4. Finally, the conclusions are drawn in Section 5.

2. Multi-time scale optimal scheduling method for HPS microgrid

2.1. Description of HPS microgrid system

The structure of the grid-connected HPS microgrid in this study is shown in **Figure 1**. The entire system consists of a small hydropower station, distributed photovoltaic (PV) generation units, a hybrid energy storage system, and user loads. Given the high randomness and volatility of hydropower and PV output, the hybrid energy storage system includes two components: Batteries and supercapacitors. The batteries are served as energy-type storage devices, which can store a large amount of electrical energy and are suitable for power response with slow changes. On the other hand, the supercapacitors are power-type storage devices, which are capable of rapid charging and discharging, to provide a fast response to power fluctuations. Both batteries and supercapacitors leverage the complementary advantages of power variation.

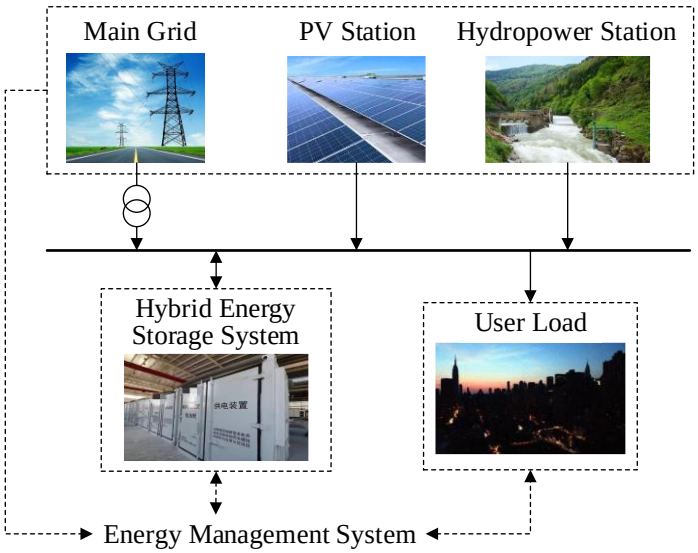

Figure 1. Structure of the HPS microgrid.

In the grid-connected mode of the HPS microgrid, if there is still surplus hydro-PV power output after meeting the load at a certain moment, the excess power will be stored in the battery. If the hydro-PV power output is insufficient to meet the load demand, it is necessary to consider purchasing electricity from the external network. If the hydro-PV output meets the load demand and the battery for energy storage is fully charged, the remaining power can be sent into the main grid. Based on the above,

the optimal scheduling problem of the HPS microgrid is grounded in the uncertain representative scenarios of PV power output, hydropower output, and load demand to reasonably arrange the charging and discharging power of the hybrid energy storage system as well as the interaction power between the HPS microgrid and the external grid.

2.2. Day-ahead stochastic chance-constrained programming model

The energy-optimal scheduling model for the HPS microgrid aims to minimize the total operating costs, which include the total operation and maintenance costs of the system C_{om}, battery depreciation and degradation costs C_{B}, and the energy interaction cost between the microgrid and the main grid C_{G}. Considering the randomness and correlation of the hydropower and PV power outputs within the microgrid, the spatiotemporal correlated scenarios for hydro-PV power outputs are generated by using the scenario generation and reduction methods introduced in Section 3. This method enables the characterization of the uncertainty in hydro-PV power output, and the day-ahead optimization scheduling model is constructed as a chance-constrained programming, with the objective function as follows:

$$\min_{P_{\text{B}},P_{\text{G}}} C_{\text{total}} = \sum_{t=1}^{T}(C_{\text{om}} + C_{\text{B}} + C_{\text{G}}) \tag{1}$$

where C_{total} is the total operating cost of the HPS microgrid system, and can be calculated as follows:

$$C_{\text{om}} = \sum_{s=1}^{S} \rho_{\text{s}} [C_{\text{PV}} P_{\text{PV}}^{s}(t)\Delta t + C_{\text{HE}} P_{\text{HE}}^{s}(t)\Delta t] + C_{\text{CN}} P_{\text{B}}(t)\Delta t \tag{2}$$

$$C_{\text{B}} = [k_s(1-\eta_{\text{Bc}})P_{\text{Bc}}(t)\Delta t] + [k_s(1-\eta_{\text{Bd}})P_{\text{Bd}}(t)\Delta t] \tag{3}$$

$$C_{\text{G}} = \begin{cases} C_{\text{p}}(t)P_{\text{G}}(t)\Delta t, & P_{\text{G}}(t) \geqslant 0 \\ C_{\text{s}}(t)P_{\text{G}}(t)\Delta t, & P_{\text{G}}(t) < 0 \end{cases} \tag{4}$$

here, ρ_{s} is the occurring probability corresponding to scenario s. S is the total number of scenarios. T is the number of scheduling periods. C_{PV} is the maintenance cost per unit of photovoltaic power. $P_{\text{PV}}^{s}(t)$ is the photovoltaic generation power at time t under scenario s; C_{HE} is the maintenance cost per unit of hydro power; $P_{\text{HE}}^{s}(t)$ is the output power of small hydropower station at time t under scenario s; C_{CN} is the maintenance cost per unit of battery charging and discharging power; $P_{\text{B}}(t)$ is the charging and discharging power of the battery at time t; k_{s} is the coefficient of battery depreciation and degradation cost; η_{Bc} and η_{Bd} are the charging and discharging efficiencies of the battery, respectively; $P_{\text{Bc}}(t)$ and $P_{\text{Bd}}(t)$ are the charging and discharging power of the battery, respectively; $C_{\text{p}}(t)$ and $C_{\text{s}}(t)$ are the purchasing and selling electricity prices at time t for HPS microgrid system; $P_{\text{G}}(t)$ is the

interaction power between the HPS microgrid system and the main power grid at time t.

The established day-ahead stochastic optimization of the HPS microgrid needs to satisfy the following constraints:

(1) Power balance constraint

$$\Pr\{P_{\mathrm{G}}(t)-P_{\mathrm{B}}(t)+P_{s}^{\mathrm{PV}}(t)+P_{s}^{\mathrm{HE}}(t)\geqslant P_{\mathrm{L}}(t)\}\geqslant \vartheta \tag{5}$$

where $\Pr\{\cdot\}$ represents the occurring probability of the event; $P_{\mathrm{L}}(t)$ denotes the user load at time t; ϑ is the confidence level of the chance constraint. Stochastic chance constraint programming adopts the principle that the final decision is allowed to fail to satisfy the constraint to a certain extent (i.e., the constraint of unfavorable cases is not satisfied), while ensuring that the probability of the constraint being valid is not less than a certain confidence level. The chance-constrained programming does not meet the constraint conditions and does not incur any penalty. There is no need to introduce compensation, but the constraint conditions are established with a certain probability, thus reducing the conservatism of constraints and better realizing decision-making under uncertain conditions.

(2) Upper and lower limit constraint of battery power

$$P_{\mathrm{B,max}}^{\mathrm{d}}\leqslant P_{\mathrm{B}}(t)\leqslant P_{\mathrm{B,max}}^{\mathrm{c}} \tag{6}$$

where $P_{\mathrm{B,max}}^{\mathrm{d}}$ and $P_{\mathrm{B,max}}^{\mathrm{c}}$ are the maximum discharging power and maximum charging power of the battery, respectively.

(3) State of charge constraint of battery

$$S_{\mathrm{B}}^{\min}\leqslant \frac{E_{\mathrm{B}}(t)}{E_{\mathrm{BA}}(t)}\leqslant S_{\mathrm{B}}^{\max} \tag{7}$$

where $S_{\mathrm{B}}^{\min}$ and $S_{\mathrm{B}}^{\max}$ are the lower and upper limits of the battery state of charge, respectively. $E_{\mathrm{BA}}(t)$ is the actual capacity of the battery at time t. $E_{\mathrm{B}}(t)$ denotes the energy storage of the battery at time t, and can be calculated as:

$$E_{\mathrm{B}}(t)=\begin{cases} E_{\mathrm{B}}(t-1)-P_{\mathrm{B}}(t)\Delta t\eta_{\mathrm{Bc}}, & P_{\mathrm{B}}(t)>0 \\ E_{\mathrm{B}}(t-1)-\dfrac{P_{\mathrm{B}}(t)\Delta t}{\eta_{\mathrm{Bd}}}, & P_{\mathrm{B}}(t)\leqslant 0 \end{cases} \tag{8}$$

(4) Purchasing and selling power constraint

$$P_{\mathrm{G,min}}\leqslant P_{\mathrm{G}}(t)\leqslant P_{\mathrm{G,max}} \tag{9}$$

where $P_{\mathrm{G,min}}$ and $P_{\mathrm{G,max}}$ are the lower and upper limits of the interaction power between the HPS microgrid system and the main grid, respectively.

2.3. Intraday power compensation model

Considering the impact of potential scenario errors in hydro-PV outputs during the day-ahead scheduling stage, the intraday rolling optimization of the HPS microgrid

firstly assesses whether the day-ahead scheduling strategy can track the output within 4 h based on ultra-short-term forecast values. If the day-ahead strategy cannot effectively track the output, a deterministic intraday power compensation model is constructed with the objective of minimizing power adjustment costs. The objective function is calculated as:

$$\min_{P_{\mathrm{B}},P_{\mathrm{G}},P_{\mathrm{sc}}} C_{\mathrm{in}} = \sum_{t=1}^{T_{\mathrm{in}}} [\lambda_{\mathrm{B}} \Delta P_{\mathrm{B}}(t) + \lambda_{\mathrm{G}} \Delta P_{\mathrm{G}}(t) + C_{\mathrm{sc}}(t)] \tag{10}$$

where C_{in} denotes the intraday power adjustment cost of the HPS system. λ_{B} and λ_{G} are the cost coefficients for the battery power adjustment and interaction power adjustment with the main grid, respectively. $\Delta P_{\mathrm{B}}(t)$ and $\Delta P_{\mathrm{G}}(t)$ denote adjustment amounts for the battery power and the interaction power with the main grid at time t, respectively. $C_{\mathrm{sc}}(t)$ is the depreciation and degradation costs of supercapacitor at time t, which is calculated as [31]:

$$C_{\mathrm{sc}} = \frac{R_{\mathrm{sc}} \Delta t}{T_{\mathrm{sc}}} \tag{11}$$

where T_{sc} is the overall lifespan of the supercapacitor. R_{sc} denotes the replacement cost of the supercapacitor. In addition to satisfying the above constraints Equations (6)–(9), the intraday optimization of the HPS microgrid system should also satisfy the following constraints:

(1) Power balance constraint

$$P_{\mathrm{L}}(t) = P_{\mathrm{PV}}(t) + P_{\mathrm{HE}}(t) + P_{\mathrm{G}}(t) - P_{\mathrm{B}}(t) - P_{\mathrm{sc}}(t) \tag{12}$$

where $P_{\mathrm{PV}}(t)$ and $P_{\mathrm{HE}}(t)$ are the ultra-short-term forecast values of PV power generation and hydropower generation at time t, respectively. $P_{\mathrm{sc}}(t)$ denotes the charging or discharging power of the supercapacitor at time t.

(2) Upper and lower limit constraint of supercapacitor power

$$P_{\mathrm{sc,max}}^{\mathrm{d}} \leqslant P_{\mathrm{sc}}(t) \leqslant P_{\mathrm{sc,max}}^{\mathrm{c}} \tag{13}$$

where $P_{\mathrm{sc,max}}^{\mathrm{d}}$ and $P_{\mathrm{sc,max}}^{\mathrm{c}}$ are the maximum discharging power and maximum charging power of supercapacitor, respectively.

(3) State of charge constraint of supercapacitor

$$S_{\mathrm{sc}}^{\min} \leqslant \frac{E_{\mathrm{sc}}(t)}{E_{\mathrm{sc,r}}(t)} \leqslant S_{\mathrm{sc}}^{\max} \tag{14}$$

where $S_{\mathrm{sc}}^{\min}$ and $S_{\mathrm{sc}}^{\max}$ are the lower and upper limits of the supercapacitor state of charge, respectively. $E_{\mathrm{sc,r}}(t)$ is the actual capacity of the supercapacitor at time t. $E_{\mathrm{sc}}(t)$ denotes the energy storage of the supercapacitor at time t, and can be calculated as:

$$E_{\mathrm{sc}}(t)=\begin{cases} E_{\mathrm{sc}}(t-1)-P_{\mathrm{sc}}(t)\Delta t\eta_{\mathrm{scc}}, & P_{\mathrm{sc}}(t)>0 \\ E_{\mathrm{sc}}(t-1)-\dfrac{P_{\mathrm{sc}}(t)\Delta t}{\eta_{\mathrm{scd}}}, & P_{\mathrm{sc}}(t)\leqslant 0 \end{cases} \tag{15}$$

where η_{scc} and η_{scd} are the charging and discharging efficiencies of the supercapacitor, respectively.

2.4. Real-time optimization scheduling

In the real-time optimization scheduling of the hydro-photovoltaic-storage microgrid, the current measured photovoltaic power, hydropower, and state of charge of the energy storage system are used to determine whether the current energy storage operation strategy can track the reported power of the hydro-photovoltaic-storage system. If it cannot track, efforts are made to minimize the difference between the combined output of the hydro-photovoltaic-storage system and the target output within the operating constraints of the energy storage system. The specific process is illustrated in **Figure 2**.

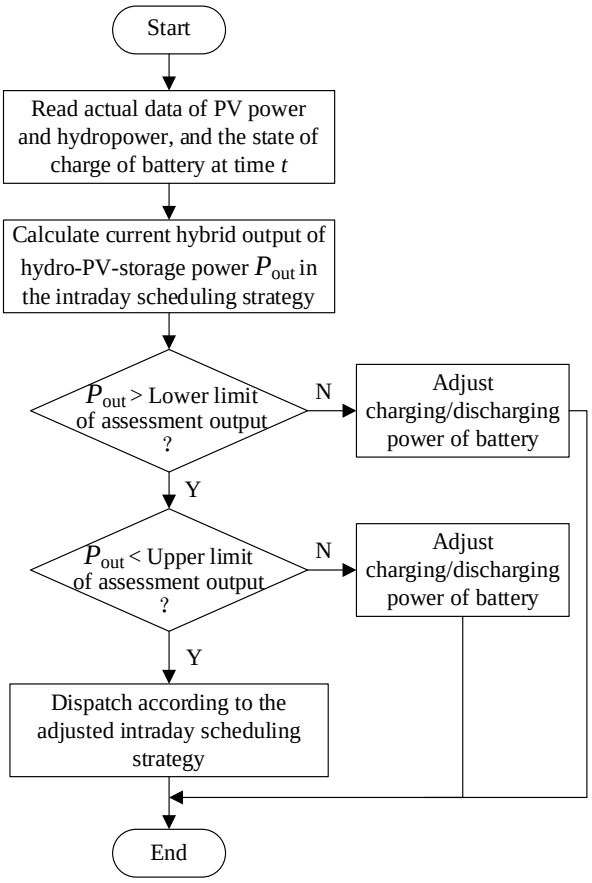

Figure 2. Real-time scheduling process of HPS microgrid.

Firstly, the actual data of PV power $P_t^{\mathrm{PV,real}}$ and hydropower $P_t^{\mathrm{HE,real}}$ at the current time t are input into the real-time scheduling process, as well as the state of charge of battery SOC_t^{real}. The battery's maximum charging power $P_t^{B,\mathrm{ch,max}}$ and the maximum

discharging power $P_t^{B,\mathrm{dis,max}}$ at current time t are calculated based on SOC_t^{real}. The combined power output of hydro-PV-storage can be calculated based on $P_t^{\mathrm{PV,real}}$, $P_t^{\mathrm{HE,real}}$ and the obtained intraday rolling optimization strategy. If the current combined output P_{out} is less than the lower limit of assessment output, it indicates that the hydro-PV-storage output is low and the discharging power of the battery is necessary to be increased. If the current combined output P_{out} exceeds the upper limit of assessment output, it indicates that the hydro-PV-storage output is high, and the charging power of the energy storage system needs to be increased. If the current combined output P_{out} falls within the range of assessment output, the obtained optimization strategy can be conducted in the real-time scheduling process.

2.5. Multi-timescale rolling optimization based on MPC

MPC is a model-based closed-loop optimization control strategy, and the core idea is rolling optimization in a finite time domain. Considering that the scenario errors of hydropower and PV power output decrease with the shortening of the time scale, the optimization scheduling of HPS microgrids is divided into three stages: 1) Day-ahead stochastic optimization; 2) intraday power compensation optimization; and 3) real-time rolling correction. A multi-time scale rolling optimization scheduling framework for HPS microgrids is established, as shown in **Figure 3**.

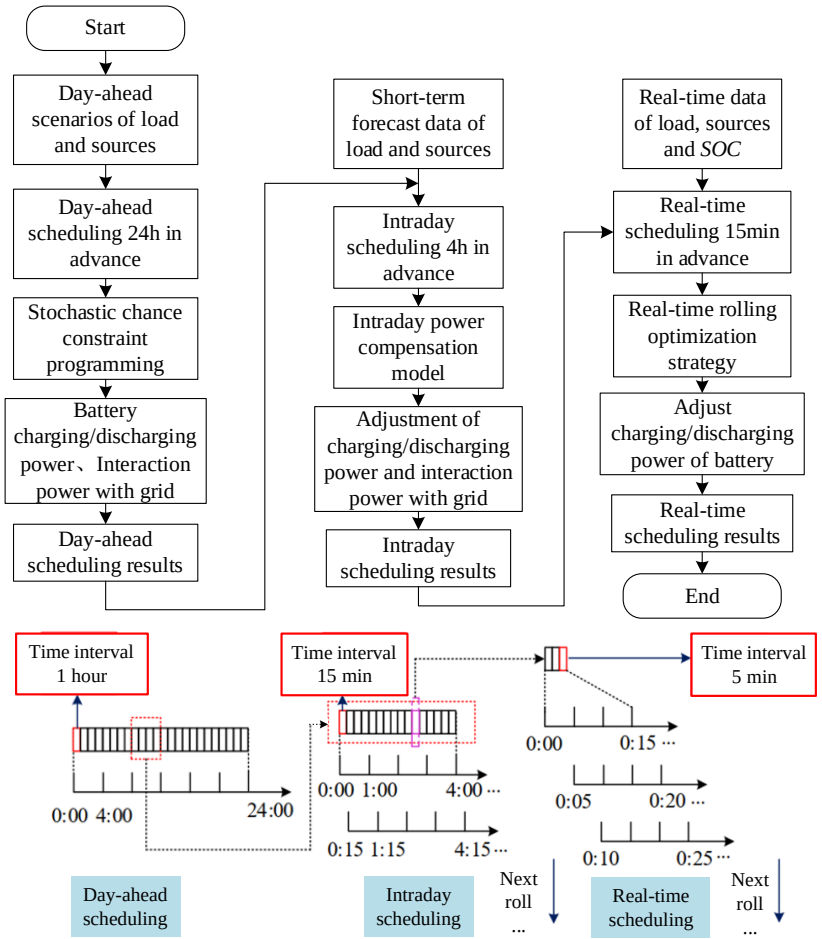

Figure 3. Multi-time scale rolling optimization framework for HPS microgrid.

In the day-ahead stochastic scheduling stage, a scheduling plan is developed 24 h in advance based on the typical scenario set of hydro-PV power with a time interval of 1h. With the lowest total operating cost of the system as the optimization goal, the charging and discharging power of the battery and the interactive power with the main grid are optimized for scheduling, and the scheduling plan for each hour of the next day is formulated. Then, the plan is released in advance as a definite value so that the operation state of each piece of equipment in the HPS microgrid is regulated according to the reference plan in the day-ahead scheduling stage.

In the intraday power compensation scheduling stage, in order to eliminate the deviation between the day-ahead reference plan and the actual intraday scheduling plan caused by scenario errors as far as possible, the intraday scheduling plan is updated every 15 min. Each rolling optimization inputs the ultra-short-term forecasting information of load, PV and hydropower outputs over the subsequent time periods. The revised 4-hour scheduling plan is optimized using MPC, with the objective of minimizing the power adjustment costs, resulting in an adjusted plan for the charging/discharging power of supercapacitors and interaction power with the main grid for the corresponding time period. Only the revised plan for the next time period is issued at this time interval. When the next scheduling cycle arrives, the above process is repeated to determine the intraday scheduling plan, which is then used as deterministic inputs in the real-time scheduling stage.

In the real-time scheduling stage, the scheduling plan is updated every 5 min based on the real-time information of renewable sources and load. After each rolling optimization, the scheduling plan is optimized for the next 15 min to correct the deviation between the previous intraday scheduling plan and the real-time conditions, modifying the charging and discharging power and interaction power. Through the MPC-based rolling optimization and feedback correction, the impact of uncertain hydropower and photovoltaic outputs on the reliable and stable operation of the microgrid is mitigated.

3. Representative scenario generation and reduction method

3.1. Scenario generation for correlated hydro-PV power

In this study, due to the non-normal probabilistic distribution for hydropower and PV power output, as well as the spatial and temporal correlations between renewable sources, the original distribution space should firstly be mapped to an independent standard normal distribution space to obtain discrete samples [32]. Afterwards, Cholesky decomposition and inverse transformation can be used to generate multivariate scenarios with specific correlations [33]. Suppose that $\mu_i\ (i=1,\cdots,m)$ denotes the m random variables, such as hydropower and PV power output, corresponding to various units; Λ_μ is the correlation matrix of the random variables. The specific scenario generation process can be summarized as follows:

1) Transform Λ_μ into the standardized correlation matrix Λ_v using the numerical search algorithm in Qin et al. [33]. Here, $v_i\ (i=1,\cdots,m)$ is consistently following a standard normal distribution;

2) Produce several n-dimensional samples whose elements follow a standard normal distribution and are independent of each other for each vector *V*;
3) Adopt Cholesky decomposition to factorize Λ_υ as $\Lambda_\upsilon = \Sigma\upsilon\Sigma_\upsilon^\top$ and obtain the correlated samples following normal distribution based on $\upsilon = \Sigma_\upsilon V$. Here, the elements in *V* are consistent with the correlations in Λ_υ;
4) Suppose that $F_{\mu_i}^{-1}$ is the inverse function and $\Phi(\upsilon_i)$ denotes the corresponding non-normal cumulative distribution of υ_i, the correlated scenarios of μ_i can be generated from the resultant υ_i in Step (3) based on the inverse transformation $\mu_i = F_{\mu_i}^{-1}[\Phi(\upsilon_i)]$ $(i = 1, \cdots, m)$.

3.2. Multivariate scenario reduction considering hydro-PV correlations

Due to the fact that the computational complexity of solving the stochastic programming model largely depends on the number of scenarios being studied, it is necessary to use scenario reduction methods to eliminate possible redundancies in the generated scenarios, thereby improving the efficiency of problem solving, especially in the large-scale systems. Unlike traditional probability distance-based scenario reduction techniques, this paper proposes an optimization-based scenario reduction model to determine the most representative scenario from the original scenario set. The goal is to maximize the sum of probability similarities between the original and reduced sets in the statistical space while minimizing the sum of correlation loss in both spatial and temporal scales after scenario reduction. The corresponding mathematical description is constructed as follows:

$$\begin{aligned} &\max_{I_{\tilde{\tau}}, \tilde{S}_{\tilde{\tau}}} \sum_{\tilde{\tau} \in \tilde{\Omega}_1} \sum_{\tau \in I_{\tilde{\tau}}} \left[Sim\left(s_\tau, \tilde{s}_{\tilde{\tau}}\right) - \beta corrloss_{S,T}\left(s_\tau, \tilde{s}_{\tilde{\tau}}\right) \right] \\ &\text{s.t.} \bigcup_{s_\tau, \tilde{s}_{\tilde{\tau}}} I_{\tilde{\tau}} = \Omega_1, \\ &\sum_{\tau \in \Omega_1} p_\tau = 1, \\ &I_{\tilde{\tau}} \cap I_{\tilde{\tau}'} = \varnothing, \ \forall \tilde{\tau} \neq \tilde{\tau}', \ \tilde{\tau}, \tilde{\tau}' \in \tilde{\Omega}_1 \end{aligned} \tag{16}$$

where Ω_1 denotes the original scenario set with the size of N_1. Ω_1 consists of the original scenario s_τ with the corresponding occurring probability p_τ. τ is the scenario node in Ω_1, and the correlation matrices in the spatial and temporal scales are $\Lambda_{\mu,\,space}$ and $\Lambda_{\mu,time}$, respectively. $\tilde{\Omega}_1$ is the reduced scenario set with the size of $\tilde{N}_1$. $\tilde{\Omega}_1$ consists of the preserved scenario $\tilde{s}_{\tilde{\tau}}$ corresponding to the occurring probability $\tilde{p}_{\tilde{\tau}}$. $\tilde{\tau}$ is the scenario node in $\tilde{\Omega}_1$. For $\tilde{\Omega}_1$, the correlation matrices in the spatial and temporal scales are $\tilde{\Lambda}_{\mu,\,space}$ and $\tilde{\Lambda}_{\mu,time}$, respectively. $I_{\tilde{\tau}}$ is the clustering subset divided by τ. The node $\tilde{\tau}$ can then be adopted to substitute the original nodes in $I_{\tilde{\tau}}$. Moreover, $Sim(\cdot)$ in Equation (16) denotes the probability similarity function, which is presented in Hu and Li [24] and used to measure the similarity degree of the reduced scenarios and the original scenarios, which can be calculated as follows:

$$Sim(s_i, s_j) = \frac{1}{n}\left[\sum_{k=1}^{n}\left(1 - \frac{p_i p_j}{p_i + p_j}\frac{|s_i^k - s_j^k|}{\left|\max\limits_{1\leqslant l\leqslant n}\{s_l^k\} - \min\limits_{1\leqslant l\leqslant n}\{s_l^k\}\right| + \varepsilon}\right)\right] \quad (17)$$

where k $(k=1, \cdots, n)$ corresponds to the *k*-th random variable in the scenario vector s_i (corresponding to the occurring probability p_i) and s_j (corresponding to the occurring probability p_j) of the n-dimensional scenario set with the size of N_1. ε is a very small constant that prevents molecules of fractions from being divided by 0. The larger the value of *Sim*, the greater the probability of similarity between the reduced scenarios and the original scenarios in the overall probability space.

Furthermore, $corrloss_{S,T}(\cdot)$ in Equation (16) denotes the correlation loss in both spatial and temporal scales between the preserved scenario set and the initial scenario set. It can be calculated as the sum of squares of the upper triangular elements in the spatial and temporal correlation deviation matrices $\Delta\Lambda_{spatial}$ and $\Delta\Lambda_{temporal}$, which are based on the calculation of Pearson correlation coefficients. In previous studies [24], it is known that the correlation between multiple random variables can nontrivially change the structure of the feasible region in MSVP so that the obtained programming results will be affected under different correlation levels. It is crucial to capture the correlation between random variables and introduce the correlations into the programming model reasonably, because even accurate solving and analyzing methods cannot compensate for the inaccurate scenario input. Therefore, the proposed metric of correlation loss in this paper is crucial, which can reflect the change of correlation before and after scenario reduction. From the perspective of approximating the solution results of MSVP before scenario reduction, it is meaningful to retain the correlation of the original scenario set (i.e., correlation loss is as small as possible), which has also been shown in the simulation analysis in the paper. Therefore, correlation loss is a good metric to characterize the multi-stochastic variable case.

Suppose the spatial dimension of hydro-PV generation units is *S*, the temporal dimension of hydro-PV power output to be considered is *T*, the calculation formula of total correlation loss can be calculated as follows:

$$\Delta\Lambda_{spatial} = \Lambda_{spatial} - \tilde{\Lambda}_{spatial} = \begin{bmatrix} 0 & \Delta\rho_{12} & \cdots & \Delta\rho_{1S} \\ \Delta\rho_{21} & 0 & \cdots & \Delta\rho_{2S} \\ \vdots & \vdots & \ddots & \vdots \\ \Delta\rho_{S1} & \Delta\rho_{S2} & \cdots & 0 \end{bmatrix} = (\Delta\rho_{ij})_{S\times S},\ (i,j=1, \cdots, S) \quad (18)$$

$$\Delta\Lambda_{temporal} = \Lambda_{temporal} - \tilde{\Lambda}_{temporal} = \begin{bmatrix} 0 & \Delta\hat{\rho}_{12} & \cdots & \Delta\hat{\rho}_{1T} \\ \Delta\hat{\rho}_{21} & 0 & \cdots & \Delta\hat{\rho}_{2T} \\ \vdots & \vdots & \ddots & \vdots \\ \Delta\hat{\rho}_{T1} & \Delta\hat{\rho}_{T2} & \cdots & 0 \end{bmatrix} = (\Delta\hat{\rho}_{ij})_{T\times T},\ (i,j=1, \cdots, T) \quad (19)$$

$$corrloss_{S,T}(s, \tilde{s}) = \sum_{i=1}^{S-1}\sum_{j=i+1}^{S}(\Delta\rho_{ij})^2 + \sum_{i=1}^{T-1}\sum_{j=i+1}^{T}(\Delta\hat{\rho}_{ij})^2 \quad (20)$$

here, $\Lambda_{spatial}$ and $\Lambda_{temporal}$ are the spatial and temporal correlation matrices of the original scenario set, respectively. $\tilde{\Lambda}_{spatial}$ and $\tilde{\Lambda}_{temporal}$ are the spatial and temporal correlation matrices of the reduced scenario set, respectively. ρ_{ij} is the spatial Pearson correlation coefficient of various renewable energy sources, and $\hat{\rho}_{ij}$ is the autocorrelation coefficient in the temporal scale of each unit. The value of $corrloss_{S,T}(s,\tilde{s})$ represents the deviation degree of spatial and temporal correlations between the preserved scenarios s in $\tilde{\Omega}_1$ and the original scenarios $\tilde{s}$ in Ω_1. The smaller the value of $corrloss_{S,T}(s,\tilde{s})$ is, the better the original correlation properties are to be preserved in $\tilde{\Omega}_1$ after the reduction operation.

β in Equation (16) denotes the correlation weight. A smaller β can select the preserved scenarios with high probability similarity but relatively large spatiotemporal correlation loss after reduction, while a larger β can ensure a high degree of correlation preservation in the original scenarios but low probability similarity. Therefore, by adjusting the value of β reasonably, an appropriate balance can be achieved between the two objectives in the scenario reduction process. In general, β takes the value of 0.5 to make a balance of the two goals. Then, the representative scenarios can be produced by conducting the following reduction operations:

1) Calculate the probability similarity matrix $SIM_{N_1\times N_1}$. Each element $SIM(i,j)$ in the matrix corresponds to the probability similarity $Sim(s_i,s_j)$ of the original scenarios s_i and s_j by Equation (17);
2) Compute the spatiotemporal correlation loss after reducing the scenarios s_i and s_j by Equations (18)–(20), and then the correlation loss matrix $CorrLoss_{N_1\times N_1}$ can be obtained by $CorrLoss(i,j)=corrloss(s_{(s_i,s_j)},\tilde{s})$. The preserved scenarios $\tilde{s}$ without s_i and s_j is in reference to the original scenarios $s_{(s_i,s_j)}$;
3) Normalize the elements in $SIM_{N_1\times N_1}$ and $CorrLoss_{N_1\times N_1}$ based on Equations (21) and (22), and obtain matrices $SIM'_{N_1\times N_1}$ and $CorrLoss'_{N_1\times N_1}$;

$$SIM'(i,j)=\frac{Sim(s_i,s_j)-SIM_{\min}}{SIM_{\max}-SIM_{\min}} \tag{21}$$

$$CorrLoss'(i,j)=\frac{corrloss(s_i,s_j)-CorrLoss_{\min}}{CorrLoss_{\max}-CorrLoss_{\min}} \tag{22}$$

4) Construct the comprehensive objective matrix $SIMCorr_{N_1\times N_1}$ by $SimCorr(i,j)=SIM'(i,j)-\beta CorrLoss'(i,j)$;
5) Find the optimal scenario pair (s_i,s_j) to be reduced corresponding to the maximum value in $SIMCorr_{N_1\times N_1}$;
6) As illustrated in **Figure 4**, merge the two optimal scenarios s_i (with probability p_i) and s_j (with probability p_j) into a new scenario s_{new} (with probability p_{new}) based on the optimal redistribution rule as follows [24]:

$$s_{new} = \frac{p_i s_i + p_j s_j}{p_i + p_j} \tag{23}$$

$$p_{new} = p_i + p_j \tag{24}$$

7) Replace the selected scenario pair (s_i, s_j) to s_{new} and the preserved scenario set $\tilde{\Omega}_1$ is refined. The size of $\tilde{\Omega}_1$ is then be decreased by one;
8) Conduct the iterative reduction on the scenario set and go back to Step (1) until the size of $\tilde{\Omega}_1$ is equal to the prespecified value $\tilde{N}_1$.

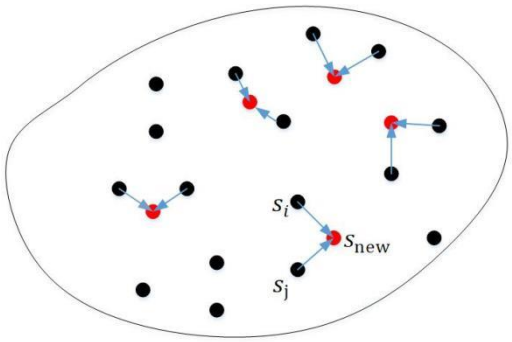

Figure 4. Illustration of optimal redistribution rule for scenario reduction.

The solution process of model (16) is similar to the process of solving scenarios with minimized Kantorovich distance in fast forward selection and simultaneous backward reduction in Heitsch and Römisch [18]. It is a recursive process. As the scale of the scenario set increases, especially for thousands of scenarios, the complexity of solving the reduction model will be greatly increased. The advantages and significance of the proposed method are more focused on the fact that the solution results by our method can achieve a closer accuracy to the solution results obtained in the original scenario set under the same degree of reduction (cutting down the same number of scenarios) compared with other methods.

4. Results and analysis

In this section, the basic data description and parameter settings for the HPS microgrid scheduling are firstly provided. Then, the performance of representative scenarios obtained by the proposed spatiotemporal scenario reduction method is compared with several typical methods. Finally, the HPS microgrid scheduling results of the constructed multi-time scale optimization model are analyzed in detail.

4.1. Data description and parameter settings

In the case study, the HPS microgrid system consists of two photovoltaic generator units, a small hydropower generator unit, a battery energy storage device, a supercapacitor energy storage device, and user loads. In grid-connected mode, the HPS microgrid can interact with the main grid for energy exchange, selling or purchasing electrical energy. The total capacity of the battery energy storage device is 200 kWh, with a rated charging and discharging power of 20 kW, and maximum and

minimum state of charge (SOC) values of 0.9 and 0.1, respectively. The charging/discharging efficiency is 82%, and the unit energy degradation cost for the battery is 6000 ¥/kWh. The supercapacitor energy storage device has a total capacity of 150 kWh, a rated charge and discharge power of 10 kW, and maximum and minimum SOC values of 0 and 1, respectively. The charging/discharging efficiency is 92%, and the unit energy degradation cost for the supercapacitor is 36,000 ¥/kWh. The upper and lower limits of the interaction power between the HPS microgrid system and the main grid are ±300 kW. During peak hours 8:00–16:00 and 18:00–22:00, the purchase and sale prices of electricity are 1.322 ¥/kWh and 0.661 ¥/kWh, respectively. During off-peak hours 6:00–8:00 and 16:00–18:00, the purchase and sale prices are 0.832 ¥/kWh and 0.416 ¥/kWh, respectively. During the valley period 22:00–6:00, the purchase and sale prices are 0.369 ¥/kWh and 0.185 ¥/kWh, respectively. The confidence level for the day-ahead stochastic chance constraint ϑ is set to 0.8.

The proposed optimal scheduling model for the HPS microgrid based on stochastic chance constraints is constructed using MATLAB and solved using the Genetic Algorithm toolbox and CPLEX solver. All experiments are implemented on a DELL PC equipped with an Intel Core i7-6700 CPU(3.4GHz) and 8GB of RAM.

4.2. Evaluation of scenario reduction results

During the day-ahead stochastic scheduling stage of HPS microgrid, based on historical data of hydropower, PV power output and user load, 50 representative scenarios with spatial and temporal correlations are produced through the initially generated scenario set with the size of 1000 and the proposed scenario reduction method. The time-series scenario of the net load power for the HPS microgrid is calculated and shown in **Figure 5**.

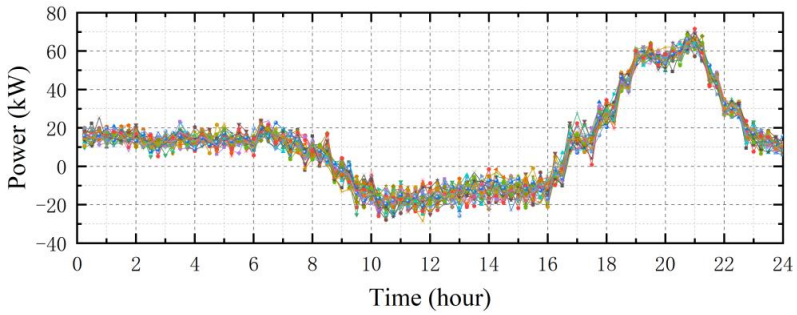

Figure 5. Representative scenarios of daily net load of HPS microgrid.

In order to evaluate the performance of the proposed scenario reduction method, the statistical deviations (e.g., mean, standard deviation, median, skewness and kurtosis) between the reduced scenario set and the original scenario set by our method are compared with the results of other typical reduction methods, including FFS [18], SBR [18], and Sim&Corrloss [24]. Different from the Sim&Corrloss method, the proposed method reasonably takes both spatial and temporal correlations into account in the calculation of the correlation loss function, thereby preserving the specific correlation characteristics of original scenarios in the reduction process. As the degree of scenario reduction increases, the physical characteristics of the reduced scenario set will inevitably deviate from the original scenario set. From the comparative statistical

deviation results in **Table 1**, compared with other methods, the proposed method can always achieve the smallest deviation between the reduced scenario set and the original scenario set for various statistical indicators. It can indicate that the introduction of a spatiotemporal correlation loss term in the comprehensive reduction model can effectively preserve the essential characteristics of the scenarios, thus having more advantages in preserving the statistical features of the scenario input space for solving the HPS microgrid stochastic scheduling model.

Table 1. Statistical deviation results of the reduced scenarios under different methods.

Statistics	FFS [18]	SBR [18]	Sim&Corrloss [24]	The proposed method
Mean	0.538	0.349	0.265	0.224
St. dev	0.240	0.187	0.159	0.086
Median	0.916	0.705	0.433	0.271
Skewness	0.393	0.352	0.314	0.280
Kurtosis	0.759	0.643	0.372	0.311

Moreover, the comparative results of the decision deviation degrees in the reduced scenarios under different methods are listed in **Table 2**. The decision deviation degree (i.e., the battery power and the interaction power with the main grid) obtained by using the proposed method is the lowest among the four methods. It indicates that compared with other scenario reduction methods, using a probability similarity function and comprehensive spatial-temporal correlation loss for scenario fusion can better ensure that the decision output is correct and effective as much as possible. On this basis, the deviation degree of the objective function value (i.e., total scheduling cost) obtained by the proposed method is the closest to the actual objective value before reduction among these methods, indicating that preserving the correlation between hydro-PV power outputs in the reduced scenario can greatly improve the approximation effect of the objective function value of the decision output space. It is necessary to consider both temporal and spatial correlation characteristics in the scenario reduction process. Therefore, the comprehensive scenario reduction method proposed in this paper is effective and can make the decision results for HPS microgrid scheduling more accurate and reliable.

Table 2. Decision deviation degrees of the reduced scenarios under different methods.

Decisions	FFS [18] (%)	SBR [18] (%)	Sim&Corrloss [24] (%)	The proposed method (%)
P_{B}	12.584	10.197	4.263	3.170
P_{G}	11.526	9.905	5.814	3.452
C_{total}	9.242	8.481	4.153	2.637

4.3. Comparative analysis of microgrid scheduling

To verify the effectiveness of the proposed optimal scheduling method for the HPS microgrid, the stochastic optimization method considering the uncertainty of

sources and load using chance constraints is compared with the deterministic optimization method based on the point prediction of source and load in Ju et al. [34]. The comparative results of the interactive power with the main grid, the battery charging/discharging power and the total scheduling results under different methods are shown in **Figures 6–8**, respectively.

As shown in **Figures 6** and **7**, the blue dashed line represents the power results after the day-ahead and intraday optimization scheduling, while the red solid line represents the scheduling results after real-time rolling optimization adjustments. It can be observed that the proposed method can achieve smaller power adjustments during real-time rolling optimization. During more scheduling periods, the real-time power adjustment amounts of the proposed method are nearly negligible. It indicates that using stochastic chance constraints to address the uncertainty of hydro-PV output can effectively enhance the robustness of day-ahead scheduling results. As for the deterministic scheduling method in Ju et al. [34], the total power mismatch for the HPS microgrid scheduling over 24 h before real-time power adjustment is 154.587 kWh. In contrast, the corresponding power mismatch amount using the proposed method is 91.813 kWh. It demonstrates that during the day-ahead stochastic optimal scheduling stage, using representative scenarios to characterize the uncertainty of hydro-PV output and adopting stochastic chance constraints in the scheduling model can significantly improve the ability of the microgrid system to deal with real-time variations of uncertain factors, thereby ensuring the stability and safety of the HPS microgrid system in the actual operation.

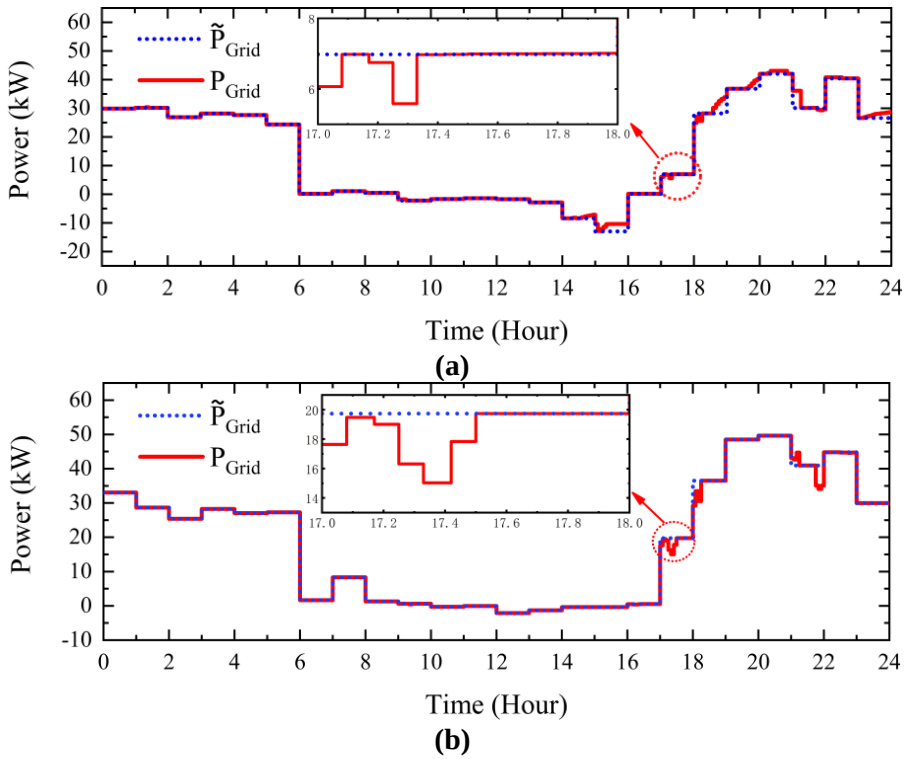

Figure 6. Comparison results of interactive power with the main grid under different methods: **(a)** Deterministic optimization method [34]; **(b)** the proposed stochastic method.

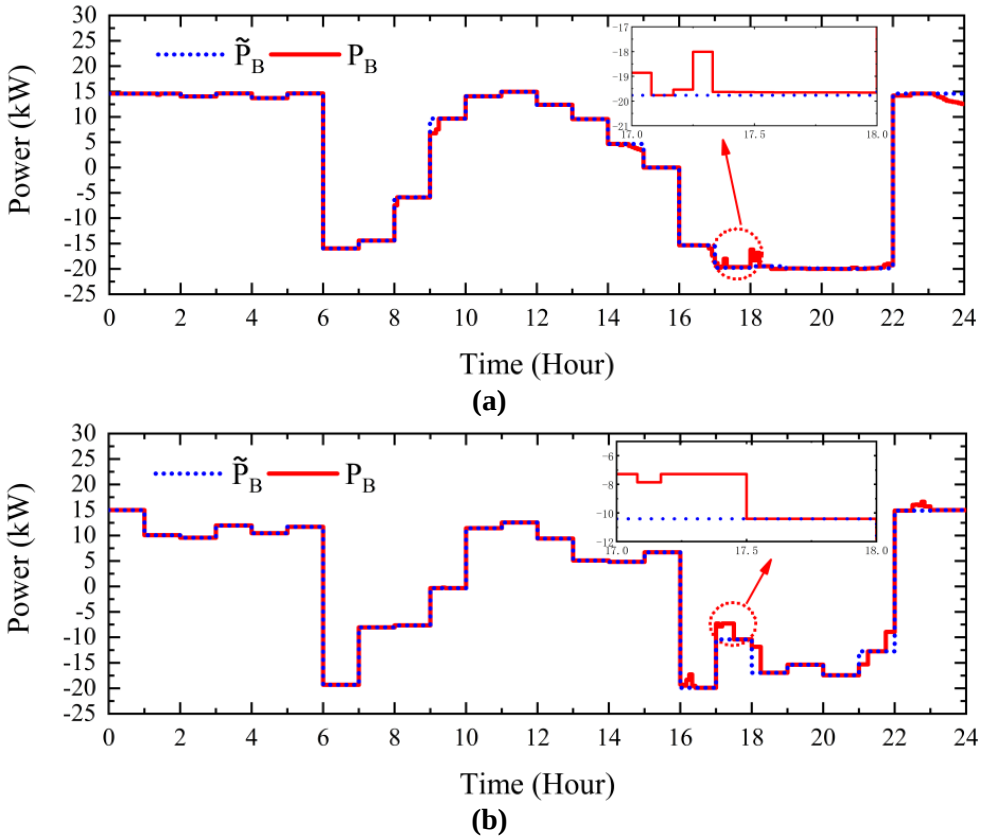

Figure 7. Comparison results of battery charging/discharging power under different methods: **(a)** Deterministic optimization method [34]; **(b)** the proposed stochastic method.

Figure 8a,b show the multi-time scale optimal scheduling results for the HPS microgrid using the deterministic method in Ju et al. [34] and the proposed method, respectively. **Table 3** lists the comparative results of the operating costs in the day-ahead and intraday stages, as well as the real-time scheduling stage, for different methods. It can be seen that the scheduling results for the charging and discharging power of the battery are influenced by electricity prices. During the low-price periods, the battery energy storage system prioritizes charging, whereas in high-price periods, the battery acts as the main power supply device and prioritizes discharging, taking advantage of the price differential to ensure the economic operation of the microgrid. Additionally, the proposed method fully considers the uncertainty of hydro-PV output as well as load. Compared to the deterministic scheduling method in Ju et al. [34], more power was purchased from the main grid during the day-ahead and intraday scheduling stages in the proposed method to ensure the feasibility of the scheduling results under various uncertain scenarios. This resulted in fewer power adjustments during the real-time scheduling stage, effectively reducing the power adjustment costs and minimizing the power fluctuations caused by scenario errors. Compared with the traditional deterministic scheduling method, the compensation power of our method can be significantly reduced by 62.774 kWh, and our power compensation cost can be significantly reduced by 144.916¥, which indicates that the proposed stochastic optimization method can effectively ensure the economy and reliability of microgrid

scheduling under uncertain conditions. Therefore, the proposed stochastic scheduling method significantly mitigates the impact of the uncertainty of hydro-PV output on the stability and economic operation of the microgrid, thereby enhancing the stability and efficiency of the HPS system under complex uncertain conditions.

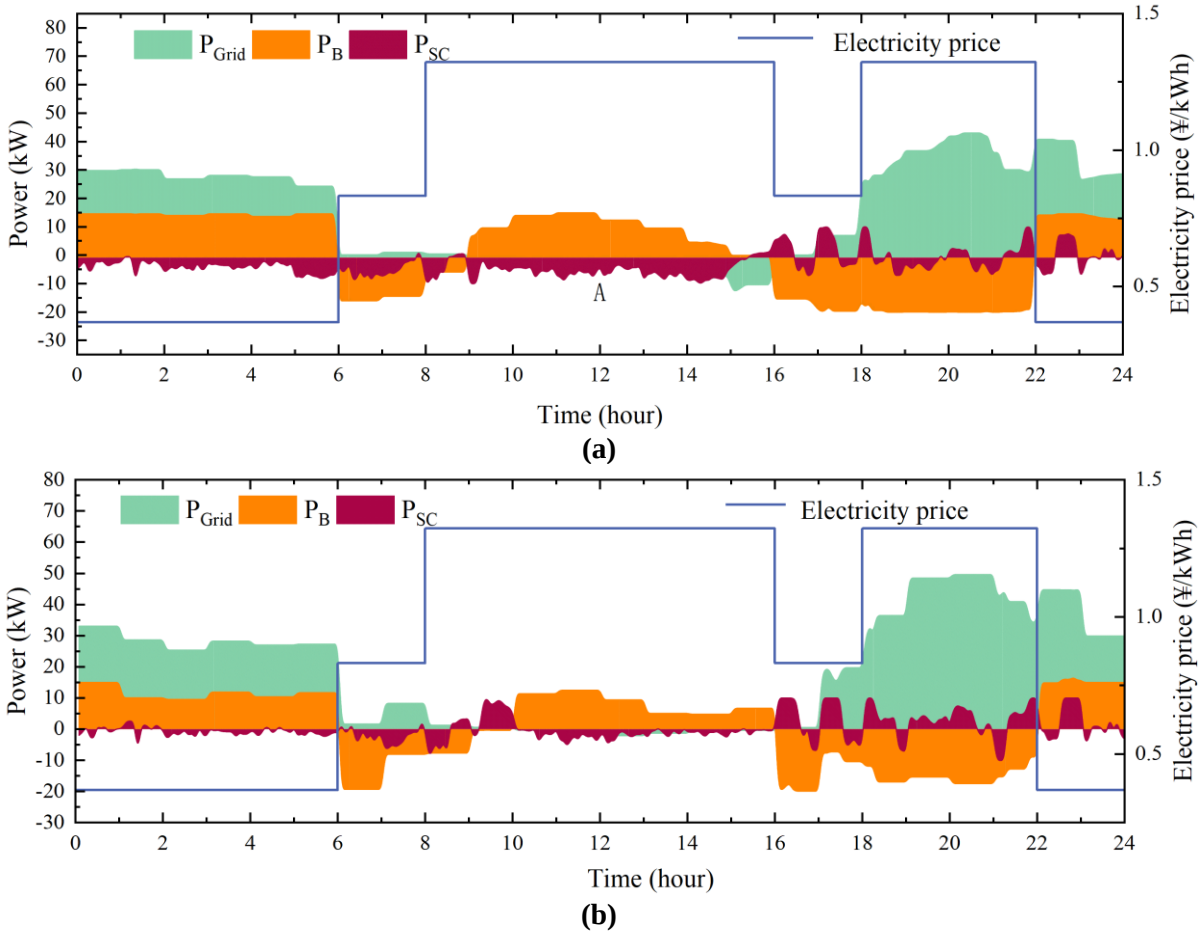

Figure 8. Comparison results of total scheduling results for HPS microgrid under different methods: **(a)** Deterministic optimization method [34]; **(b)** the proposed stochastic method.

Table 3. Comparison of operation costs of HPS microgrid under different methods.

Methods	Day-ahead & Intraday (¥)	Real-time (¥)	Total costs (¥)
Deterministic method [34]	291.674	380.501	672.175
The proposed method	357.935	169.324	527.259

5. Conclusions

To mitigate the adverse impacts of the uncertainty of hydro-PV output on the actual operation of microgrid systems, this paper proposes a rolling optimization control method for HPS microgrids based on stochastic chance constraints. By using a novel multivariate scenario reduction method to obtain the representative scenarios for hydro-PV output, a day-ahead stochastic optimization scheduling model and an intraday power compensation model are established, respectively. Then, the real-time power adjustment strategies are presented. Stochastic model predictive control is employed for multi-time-scale rolling optimization and feedback correction, aiming to

minimize the operating costs of the HPS microgrid. Experimental results of HPS microgrid scheduling indicate that compared to the traditional deterministic optimization methods, the proposed method can better deal with the uncertainty of hydro-PV output to achieve lower power compensation and operation costs. Through scenario-based stochastic optimization, multi-time-scale rolling optimization and feedback correction, it effectively suppresses the power fluctuations of various units caused by source-load uncertainty, thereby significantly improving the stability and economic efficiency of microgrid operations.

Author contributions: Conceptualization, QG and WX; methodology, QG; software, XL; validation, XL, LL and HY; formal analysis, ZW; investigation, QG; resources, XL; data curation, XL; writing—original draft preparation, QG; writing—review and editing, QG; visualization, WX; supervision, QG; project administration, QG; funding acquisition, QG. All authors have read and agreed to the published version of the manuscript.

Conflict of interest: The authors declare no conflict of interest.

References

1. Olatunde O, Hassan MY, Abdullah MP, et al. Hybrid photovoltaic/small-hydropower microgrid in smart distribution network with grid isolated electric vehicle charging system. Journal of Energy Storage. 2020; 31: 101673. doi: 10.1016/j.est.2020.101673
2. Guan Y, Vasquez JC, Guerrero JM, et al. Frequency Stability of Hierarchically Controlled Hybrid Photovoltaic-Battery-Hydropower Microgrids. IEEE Transactions on Industry Applications. 2015; 51(6): 4729–4742. doi: 10.1109/tia.2015.2458954
3. Bagheri F, Dagdougui H, Gendreau M. Stochastic optimization and scenario generation for peak load shaving in Smart District microgrid: Sizing and operation. Energy and Buildings. 2022; 275: 112426. doi: 10.1016/j.enbuild.2022.112426
4. Deng J, Li H, Hu J, et al. A new wind speed scenario generation method based on spatiotemporal dependency structure. Renewable Energy. 2021; 163: 1951–1962. doi: 10.1016/j.renene.2020.10.132
5. Zhu X, Yu Z, Liu X. Security constrained unit commitment with extreme wind scenarios. Journal of Modern Power Systems and Clean Energy. 2020; 8(3): 464–472. doi: 10.35833/mpce.2018.000797
6. Ma H, Zhang W, Wang A. A two-phase robust comprehensive optimal scheduling strategy for regional distribution network based on multiple scenarios. Frontiers in Energy Research. 2024; 12. doi: 10.3389/fenrg.2024.1496302
7. Rezaee Jordehi A, Mansouri SA, Tostado-Véliz M, et al. A tri-level stochastic model for operational planning of microgrids with hydrogen refuelling station-integrated energy hubs. International Journal of Hydrogen Energy. 2024; 96: 1131–1145. doi: 10.1016/j.ijhydene.2024.11.401
8. Azizivahed A, Gholami K, Arefi A, et al. Stochastic scheduling of energy sharing in reconfigurable multi-microgrid systems in the presence of vehicle-to-grid technology. Electric Power Systems Research. 2024; 231: 110285. doi: 10.1016/j.epsr.2024.110285
9. Seyedeh-Barhagh S, Abapour M, Mohammadi-Ivatloo B, et al. Optimal scheduling of a microgrid based on renewable resources and demand response program using stochastic and IGDT-based approach. Journal of Energy Storage. 2024; 86: 111306. doi: 10.1016/j.est.2024.111306
10. Shaillan HM, Tohidi S, Hagh MT, et al. Risk-aware two-stage stochastic short-term planning of a hybrid multi-microgrid integrated with an all-in-one vehicle station and end-user cooperation. Journal of Energy Storage. 2024; 78: 110083. doi: 10.1016/j.est.2023.110083
11. Hu J, Li H. A transfer learning-based scenario generation method for stochastic optimal scheduling of microgrid with newly-built wind farm. Renewable Energy. 2022; 185: 1139–1151. doi: 10.1016/j.renene.2021.12.110

12. Wang Z, Hu J, Liu B. Stochastic optimal dispatching strategy of electricity-hydrogen-gas-heat integrated energy system based on improved spectral clustering method. International Journal of Electrical Power & Energy Systems. 2021; 126: 106495. doi: 10.1016/j.ijepes.2020.106495
13. Abunima H, Park WH, Glick MB, et al. Two-Stage stochastic optimization for operating a Renewable-Based Microgrid. Applied Energy. 2022; 325: 119848. doi: 10.1016/j.apenergy.2022.119848
14. Li K, Yang F, Wang L, et al. A scenario-based two-stage stochastic optimization approach for multi-energy microgrids. Applied Energy. 2022; 322: 119388. doi: 10.1016/j.apenergy.2022.119388
15. Jani A, Karimi H, Jadid S. Two-layer stochastic day-ahead and real-time energy management of networked microgrids considering integration of renewable energy resources. Applied Energy. 2022; 323: 119630. doi: 10.1016/j.apenergy.2022.119630
16. Aaslid P, Korpås M, Belsnes MM, et al. Stochastic operation of energy constrained microgrids considering battery degradation. Electric Power Systems Research. 2022; 212: 108462. doi: 10.1016/j.epsr.2022.108462
17. Kizito R, Liu Z, Li X, et al. Multi-stage stochastic optimization of islanded utility-microgrids design after natural disasters. Operations Research Perspectives. 2022; 9: 100235. doi: 10.1016/j.orp.2022.100235
18. Heitsch H, Römisch W. Scenario reduction algorithms in stochastic programming. Computational Optimization and Applications. 2003; 24: 187–206.
19. Xu J, Yi X, Sun Y, et al. Stochastic Optimal Scheduling Based on Scenario Analysis for Wind Farms. IEEE Transactions on Sustainable Energy. 2017; 8(4): 1548–1559. doi: 10.1109/tste.2017.2694882
20. Pandzic H, Dvorkin Y, Qiu T, et al. Toward Cost-Efficient and Reliable Unit Commitment Under Uncertainty. IEEE Transactions on Power Systems. 2016; 31(2): 970–982. doi: 10.1109/tpwrs.2015.2434848
21. Park S, Xu Q, Hobbs BF. Comparing scenario reduction methods for stochastic transmission planning. IET Generation, Transmission & Distribution. 2019; 13(7): 1005–1013. doi: 10.1049/iet-gtd.2018.6362
22. Beltran F, de Oliveira W, Finardi EC. Application of Scenario Tree Reduction Via Quadratic Process to Medium-Term Hydrothermal Scheduling Problem. IEEE Transactions on Power Systems. 2017; 32(6): 4351–4361. doi: 10.1109/tpwrs.2017.2658444
23. Zhan J, Chung CY, Zare A. A fast solution method for stochastic transmission expansion planning. IEEE Transactions on Power Systems. 2017; 32(6): 4684–4695. doi: 10.1109/tpwrs.2017.2665695
24. Hu J, Li H. A new clustering approach for scenario reduction in multi-stochastic variable programming. IEEE Transactions on Power Systems. 2019; 34(5): 3813–3825. doi: 10.1109/tpwrs.2019.2901545
25. Hu J, Li H, Liu Z. Scenario reduction based on correlation sensitivity and its application in microgrid optimization. International Transactions on Electrical Energy Systems. 2021; 31(3). doi: 10.1002/2050-7038.12747
26. Zhang Y, Meng F, Wang R, et al. Uncertainty-resistant stochastic MPC approach for optimal operation of CHP microgrid. Energy. 2019; 179: 1265–1278. doi: 10.1016/j.energy.2019.04.151
27. Bazmohammadi N, Tahsiri A, Anvari-Moghaddam A, et al. Stochastic predictive control of multi-microgrid systems. IEEE Transactions on Industry Applications. 2019; 55(5): 5311–5319. doi: 10.1109/tia.2019.2918051
28. Jiao F, Zou Y, Zhang X, et al. Online optimal dispatch based on combined robust and stochastic model predictive control for a microgrid including EV charging station. Energy. 2022; 247: 123220. doi: 10.1016/j.energy.2022.123220
29. Lin Y, Li L, Zhang J, et al. A scenario-based stochastic model predictive control approach for microgrid operation at an Australian cotton farm under uncertainties. International Journal of Electrical Power & Energy Systems. 2024; 159: 110025. doi: 10.1016/j.ijepes.2024.110025
30. Wei S, Gao X, Zhang Y, et al. An improved stochastic model predictive control operation strategy of integrated energy system based on a single-layer multi-timescale framework. Energy. 2021; 235: 121320. doi: 10.1016/j.energy.2021.121320
31. Hu J, Yan P, Tan G. A two-layer optimal scheduling method for microgrids based on adaptive stochastic model predictive control. Measurement Science and Technology. 2025; 36(2): 026208. doi: 10.1088/1361-6501/ada39b
32. Hu J, Yan P, Tan G. Spatiotemporal dependence modeling of wind speeds via adaptive-selected mixture pair copulas for scenario-based applications. Renewable Energy. 2025; 244: 122650. doi: 10.1016/j.renene.2025.122650
33. Qin Z, Li W, Xiong X. Incorporating multiple correlations among wind speeds, photovoltaic powers and bus loads in composite system reliability evaluation. Applied Energy. 2013; 110: 285–294. doi: 10.1016/j.apenergy.2013.04.045
34. Ju C, Wang P, Goel L, Xu Y. A two-layer energy management system for microgrids with hybrid energy storage considering degradation costs. IEEE Transactions on Smart Grid. 2018; 9(6): 6047–6057. doi: 10.1109/tsg.2017.2703126